Microwave-assisted selective oxidation of sugars to carboxylic acids derivatives in water over zinc-vanadium mixed oxide

Khadija Khallouk, Abderrahim Solhy, Najlae Idrissi, Valérie Flaud, Abdelhak Kherbeche, Abdellatif Barakat

Microwave-assisted selective oxidation of sugars to carboxylic acids derivatives in water over zinc-vanadium mixed oxide

Khadija Khallouk,[a,b,c] Abderrahim Solhy,[c] Najlae Idrissi[d], Valérie Flaud[e], Abdelhak Kherbeche,[b] and Abdellatif Barakat[a,c*]

[a.] IATE, CIRAD, Montpellier SupAgro, INRA, University of Montpelier, France
[b.] LCME, EST, Sidi Mohammed Ben Abdellah University, 30000, Fès, Morocco
[c.] Mohammed VI Polytechnic University (UM6P). Benguerir, Morocco
[d.] University Sultan Moulay Slimane, FST Beni-Mellal, Morocco
[e.] ICGM, Institut Charles Gerhardt Montpellier, University of Montpellier, France

Corresponding author: Abdellatif.barakat@inra.fr

Abstract

Zinc-vanadium ($Zn_3V_2O_8$) nanostructured mixed oxide (ZVO) was synthesized by precipitation method. The ZVO was characterized by TGA, XRD, N_2-adsorption/desorption, NH_3-TPD, XPS, SEM, and TEM. XPS and NH_3-TPD analyses revealed that it was a Zn/V-based strong oxidant catalyst, with a mixture of both Lewis acid and Brønsted surface acid sites. The ZVO was found to be an efficient catalyst for selective oxidation of glucose and xylose to galacturonic and glycolic acid, respectively, under microwave activation. Response surface methodology was applied to find the optimal operating conditions for maximization of the sugar conversion and selectivity. There was a 60% selectivity of galacturonic acid and 46% of glycolic acid using glucose and xylose, respectively. The ability to regenerate the ZVO was assessed by determining the change in the reaction indices in successive reaction–regeneration cycles. The causes of performance activation were ascertained, characterizing the regenerated ZVO by XRD, SEM, and NH_3-TPD.

Keywords: Zinc-vanadium oxide, catalysis, oxidation, sugars, activation, microwaves, organic acids

1. Introduction

Organic acids are organic compounds that are essential in many industrial sectors[1, 2]. The food & beverages, petrochemical, pharmaceutical, textile, and adhesives industries are among the main end-users for organic acids. Organic acids are also widely used in the production of several chemicals and materials used in the automotive and construction industries[1-3]. The main organic acids in terms of annual production are citric acid, acetic acid, lactic acid, galacturonic acid, and gluconic acid[4-7]. Moreover, acetic acid is used as a food flavor enhancer and flavoring agent, acidifier, and preservative [3, 4]. On the other hand, galacturonic or uronic

acids, with either a single or two alkyl chains, are efficient, biocompatible, nonionic surfactant molecules [8-11]. A host of other synthetic uronic acid-containing entities are also of special relevance in the design of bioactive molecules such as supramolecular entities, organic synthesis, and materials chemistry[11-14]. Galacturonic acids are derived from renewable raw materials such as lignocellulosic biomass (glucuronoxylans) and fruits (pectins)[15]. These monosaccharides, which contain two appropriate functional sites (anomeric hydroxyl and carboxylic acid), are suitable starting material for reactions with nucleophilic agents (alcohols, amines, or thiols)[14, 16]. Organic acids are generally produced by fermentation of carbohydrate substrates[17, 18]. This is presently the most used route[19]. Following fermentation, various extraction and purification processes are required to obtain a product with the desired properties. The design of specific molecular building units such as organic acids is clearly a highly topical issue that is of major importance [20-22]. However, alternative chemical production processes have been considered such as the transformation of biobased compounds into chemicals [23, 24]. Thus, monosaccharides (glucose, xylose, etc.) are valuable platform chemicals that can be transformed into molecular building blocks such as organic acids [25, 26]. Several catalytic processes for the transformation of glucose and xylose have been developed to produce organic acids. Electrocatalytic[27, 28], photocatalytic[29, 30], photo electrocatalytic [31], and catalytic oxidation processes[32, 33]are of particular interest in this regard. The catalytic systems used comprise: $Ba(OH)_2$[29], $CuO\text{-}CeO_2$[34], a binary catalyst system of hetero poly acid $H_5PV_2Mo_{10}O_{40}/H_2SO_4$[35], $AlCl_3/SnCl_2$, [36],$LaCoO_3$[37],ZrO_2[38], and iron salts ($FeCl_3{\cdot}6H_2O$, $FeCl_2$, $Fe_2(SO_4)_3{\cdot}xH_2O$, $FeSO_4{\cdot}7H_2O$)[39]. There are also many examples in the literature of catalysis by noble metals dispersed on carbon supports [40-47], or porous oxides such as TiO_2[48, 49], Au/Al_2O_3, Au/CeO_2, $Au/CeO_2(20wt\%)/Al_2O_3$, $Au/CeO_2(25wt\%)/ZrO_2$ or $Au/CeO_2(50wt\%)/ZrO_2$[50], and $Pd\text{-}Te/SiO_2$ or $Pd\text{-}Te/Al_2O_3$ [51]. Marianou *et al.*[52] studied the conversion of glucose by testing four types of Sn-based catalysts, *i.e.* $SnCl_2$ and $SnCl_4$ as homogeneous catalysts or as the respective oxides in heterogeneous systems: SnO_2 supported

on γ-Al_2O_3, and $Sn^{\delta+}$/zeolites (ZSM-5 and Beta) or $Sn^{\delta+}$/Al-MCM-41 (mesoporous aluminosilicates). This chemical process was achieved mainly in biphasic (H_2O/DMSO) media. The authors compared and verified the effect of Lewis and Brønsted acidity on the selectivity of this transformation. Wenkin *et al.*[53] designed a carbon-supported bismuth-promoted palladium catalyst, which resulted in more selective oxidation of glucose to gluconic acid. Recently, Wojcieszak *et al.*[54] developed a cesium-promoted gold nanoparticle catalyst. The gold nanoparticles were supported on CeO_2 using a soft chemical reduction method with hydrazine. The Au/CeO_2 catalytic performance and efficiency were improved by promoting this catalyst by cesium (Au-Cs/CeO_2) in order to convert glucose, fructose, and maltose into glucuronic acid. The authors achieved this reaction in aqueous solution at low temperature using O_2 as the oxidant and without adding any base. There are also other reports of nanostructured bimetallic catalytic systems supported on TiO_2in the literature, such as Cu-Au/TiO_2 and Ru-Au/TiO_2[55], and Pt_1Cu_3/TiO_2[56]. Another major part of sustainable synthesis design involves the use of microwave irradiation[57, 58]. Kumar & co-workers[59], for example, used microwave irradiation to catalyze the oxidation of glucose, molasses, and sucrose into levulinic acid. The catalyst was a synergistic system based on a mixture of metal salt ($ZnBr_2$) and hydrochloric acid. The performance of this system was attributed to the in-situ formation of HBr (pKa= -9), which is stronger than HCl (pKa= -7). This is due to the size of bromine, which is larger than chlorine. The authors also studied the effect of a number of the reaction parameters in order to optimize the catalytic process. In another work, a one-pot process was developed based on microwave-assisted conversion of carbohydrate feedstock wastes into levulinic acid by the catalytic action of HCl[60]. More recently, Rautiainen *et al.*[61] reported that microwave-assisted catalytic oxidation of glucose to gluconic acid could readily be achieved by using Au-Al_2O_3 as a catalyst and hydrogen peroxide as the oxidant. The authors concluded that this process leads to a high level of conversion and selectivity with short reaction times and very high turn-over frequencies. Mixed oxides based on the transition metal vanadium, such as

$Zn_3V_2O_8$ (ZVO), are a significant category of mixed oxides that have received extensive interest, notably for their considerable potential of applications in cutting-edge technologies[62, 63]. This material can be synthesized by various methods including: sol-gel[64], hydrothermal [62], and solid-state synthesis[63]as well as by co-precipitation [65]. Recently, a facile, rapid, and solvent-free method to synthesize nanostructured ZVO has been reported[66]. The authors of this study highlighted the impact of the nature of the precursors used on the material's morphology. There have been no studies to date in the area of catalysis, except for a few publications regarding the use of this type of material in photocatalysis. Mondal *et al.*[67]used ZVO as a photocatalyst for photodegradation of several organic dye molecules under UV-light irradiation. To the best of our knowledge, no studies of the use of ZVO as a heterogeneous catalyst for the selective conversion of sugars into organic acids under microwave irradiation have been reported to date. Here, we report ZVO-catalyzed microwave-assisted selective oxidation of glucose and xylose to galacturonic and glycolic acids, respectively. Optimization of this process required the use of response surface methodology, which also corroborated this work. The freshly prepared and recovered ZVO was characterized extensively in order to allow in-depth interpretation of our concept.

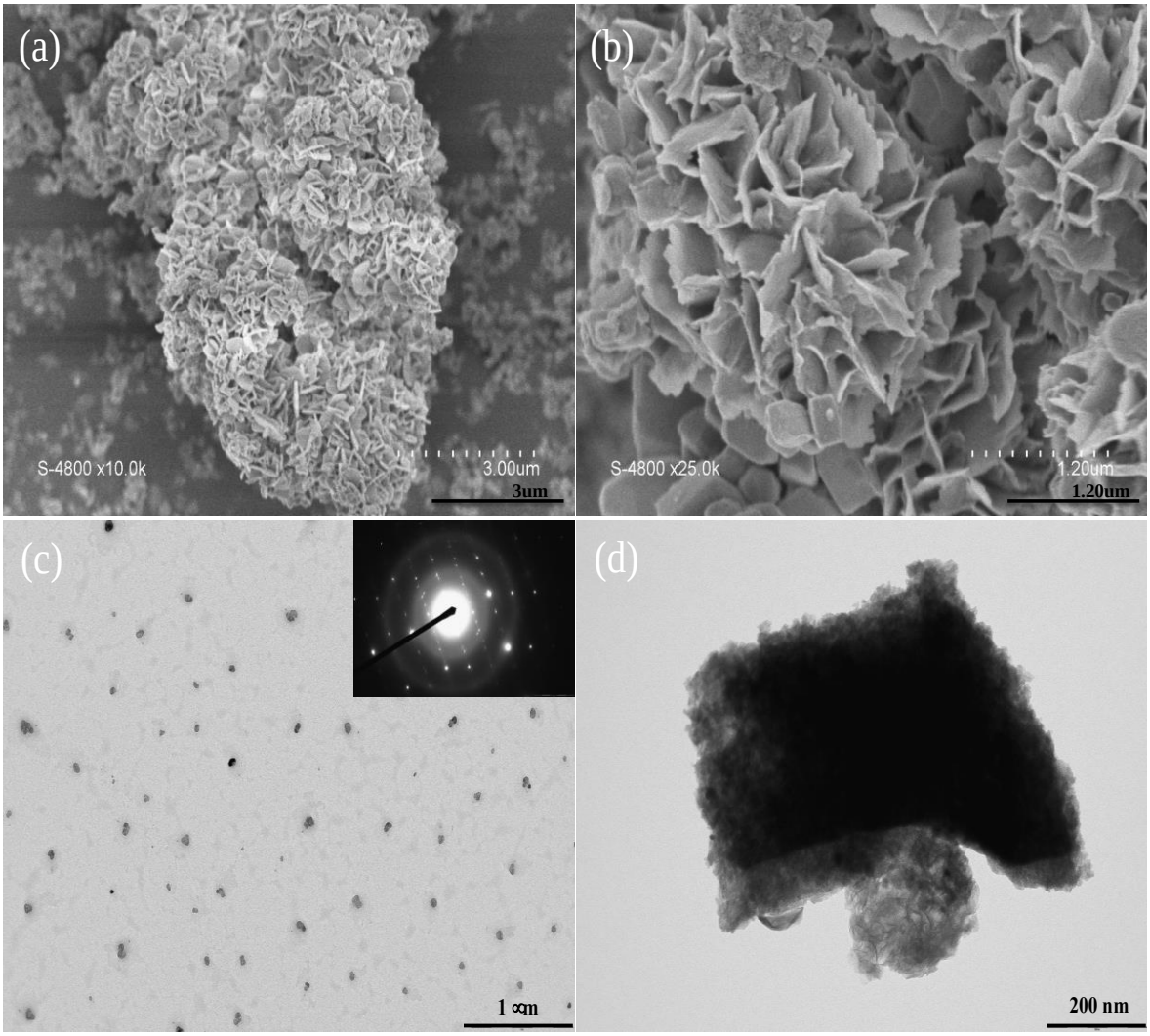

Figure 1: SEM of the ZVO at two magnifications (a & b). TEM images of the ZVO (c & d) and the corresponding electron diffraction (SAED) pattern (inset).

2. Materials and Methods

2.1. Synthesis of the zinc-vanadium mixed oxide (ZVO)

In a typical synthesis, a 0.1M aqueous solution of $ZnCl_2$ was mixed with a 0.1M aqueous solution of NH_4VO_3 in a beaker at room temperature. A concentrated solution of NH_4OH was slowly added dropwise to adjust the pH to 10. The resulting milky solution was then transferred to a reflux system and was heated for 4 hat 80 °C. After cooling to room temperature, the mixture was centrifuged, and the precipitate was washed thoroughly with deionized water to remove any residual reagents, and then vacuum dried at 80°C for 12h. The obtained powder was further calcined in a muffle furnace at 550°C with a ramp rate of 5°C/min for 4 hours.

2.2. Materials & apparatus

All of the reagents were used as received without further purification. Thermogravimetric analysis (TGA) was conducted under air in a TA Instruments Q500 device with a 10 °C/min ramp between 25 and 1,000 °C. The catalytic conversion of xylose and glucose to organic acids by microwave energy was carried out by means of a microwave oven from Strat-Synth (Milestone S.r.l.) equipped with a 16-closed-vessel position carousel. The system had an automatic temperature control with a fiber optic sensor and a maximum microwave power output of 1,200 W. The time, temperature, and power were monitored throughout the microwave process by EasyCONTROL terminal 640 software. A thermostatic vacuum dryer (Vacuo-Temp) was used to dry the materials. X-ray diffraction (XRD) patterns were obtained at room temperature with a Bruker AXS D-8 diffractometer using Cu-Kα radiation in Bragg-Brentano geometry (θ-2θ). Scanning electron microscopy (SEM) images were obtained with an FEI Quanta 200 microscope after carbon metallization. Transmission electron microscopy (TEM) was conducted with a Tecnai G2 microscope at 120 kV. Gas adsorption data in N_2 were collected using a Quantachrome Autosorb-1 automatic analyzer. Prior to N_2 sorption, all of the samples were degassed at 100°C overnight under dynamic vacuum conditions. The specific surface areas were determined from the nitrogen adsorption/desorption isotherms at 77 K using the BET (Brunauer–Emmett–Teller) method. For characterization of the acid sites on the ZVO surfaces, ammonia-temperature-programmed desorption (NH_3-TPD) analysis was carried out on an AutosorbiQ acidity analyzer. For the NH_3-TPD measurements, the samples were degassed at 100 °C under a dry He flow for 1h, and then cooled to ambient temperature. For ammonia adsorption, the degassed samples were subjected to a flow of diluted NH_3 (20%) for 30 min, and the system was allowed to equilibrate. The temperature was then raised at a heating rate of 10 °C/min up to 750 °C. The TPD experiments were typically carried out at temperatures ranging from 100 to 750 °C using a thermal conductivity detector, in a flow of dry He. The X-ray photoelectron spectroscopy (XPS) studies were carried out with an ESCALAB 250 Thermo Electron

spectrometer equipped with a monochromatic Al Kα X-ray source (hν = 1,486.6 eV). The conversion and selectivity were validated by HPLC analysis of the reaction mixture after catalytic tests. A Waters HPLC equipped with a BioRad HPX-87H column and a refractive index detector was used. For the HPLC analysis of organic acids, the mobile phase was 0.005 M H_2SO_4 (0.3 mL/min). The characteristic peaks for organic products were identified based on their retention times. Each peak was integrated, and the actual concentrations of organic products were calculated from their respective pre-calibrated plots of peak areas vs. concentrations. The selectivities were calculated based on total detected carbon yields (yield of an individual product x100)/(total yield of all products).

2.3. Catalytic oxidation of sugars into organic acids

The process of converting sugars into organic acids involved dissolving a sample (100 mg) of each sugar (glucose or xylose) in 10 mL of water in the presence of H_2O_2. ZVO was added (10 mg) and the reaction mixture was then transferred to a Teflon-sealed MW reactor and exposed to MW irradiation. The microwave power (W), temperature, and reaction time were optimized by the Box-Behnken design. After cooling to room temperature, the catalyst was separated by centrifugation, and the final mixture was analyzed by HPLC. The recovered catalyst was washed twice with dichloromethane and water, and then dried at 100 °C for 24h before being reused in subsequent reactions to assess its prolonged activity.

Table. 1. Experimental ranges and levels of independent variables

Independent variables	Symbols	Levels		
		-1	0	1
H_2O_2 (mmol)	X_1	0.012	0.106	0.2
Microwave power (W)	X_2	200	600	800
Temperature (°C)	X_3	50	75	100
Time (min)	X_4	5	17.5	30

2.4. Box-Behnken design

The significant variables such as the H_2O_2concentration (mmol), microwave power (W), temperature (°C), and time (min) were chosen as the critical variables and designated as X_1, X_2,

X_3, and X_4, respectively. The low, middle, and high levels of each variable were designated as -1, 0, and +1, respectively (Table 1). It should be emphasized that this is the reason why JMP-14 trial software was used. In a system involving four independent variables X_1, X_2, X_3, and X_4, the mathematical relationship of the response of these variables can be approximated by the quadratic (second-order) polynomial equation (**Eq. 1**):

$$Y_{conversion} = \beta_0 + \sum_{i=1}^{4} \beta_i X_i + \sum_{i=1}^{4} \beta_{ii} X_i^2 + \sum \sum_{i<j=1}^{4} \beta_{ij} X_i X_j$$

Where $Y_{conversion}$ is the predicted response variable; X_i. X_j(i=1. 4; j=1. 4; i#j) represent the coded independent variables (microwave conditions); β_0 is the intercept coefficient; $\beta_i$are the linear terms; β_{ii} are the squared terms; and $\beta_{ij}$are the interaction terms.

3. Results and Discussion

3.1. Catalyst Characterization

The thermal behavior of the dried ZVO was examined by TGA analysis under air (**Fig. S1**). The analysis clearly exhibited three steps of weight loss, while under air it decomposed in two major steps. The first weight loss at70 to 150 °C was due to water molecule desorption and the decomposition of hydroxylated derivatives. The second weight loss was at 260 to 300 °C and was due to the degradation of reagents (chloride and nitrate). The third loss above 500 °C was due to maturation and crystallization of the ZVO. As shown in **Fig. S2** (a), crystalline ZVO powder could be obtained using the precipitation method followed by calcination at 550 °C. This analysis only revealed one phase, corresponding to the orthorhombic phase of ZVO ($Zn_3V_2O_8$), which is consistent with JCPDS card No. 34-0378. The lattice parameters are: a = 8.306 Å, b = 11.540 Å and c = 6.117 Å. The peaks were relatively broad, which is characteristic of nanocrystalline particles. The XRD pattern revealed the absence of impurities and the high crystalline nature of the as-synthesized ZVO material. The BET surface area of the ZVO was 34 m^2/g and its pore volume was 0.001609 cm^3/g. The nitrogen sorption isotherm of the ZVO was type III & IV, displaying a type H3 hysteresis loop in the relative pressure range of 0.85-

0.95 and plateaus in the adsorption branches (**Fig. S3**), indicative of its intergranular porosity due to the formation of aggregates of plate-like particles forming slit-like pores. We note that the adsorbed volume remained low until P/P0 equaled 0.85, which corresponds to the constitution of a molecular monolayer. The adsorption of $N_2$was carried out progressively to generate a monolayer covering the entire external surface of the ZVO pores. Fig. 1 (a, b) shows SEM images of the ZVO at two different levels of magnification. These images of the as-obtained mixed oxide after calcination indicate a porous nano-flower morphology superstructure. These flower-like 3D formations had coarse surfaces. The TEM analysis of the ZVO revealed that the sample was well nanostructured, with an irregular morphology due to loose assembly of the particles (Fig. 1), and other images were added on SI (**Fig. S4**).We note that the ZVO nanoparticles aggregated and agglomerated with one another to form superstructures shaped by heterogeneous nucleation and growth of nanosheets, but they were well dispersed (Fig. 1c). This observation can be explained by the Ostwald ripening phenomena. The SAED patterns exhibited quasi-continuous diffraction rings (inset in Figure 1c), which is characteristic of polycrystalline nanoparticles. The surface composition and chemical states of the ZVO were studied using X-ray photoelectron spectroscopy. The survey spectrum (Fig. 2a) illustrates the chemical composition of the as-prepared ZVO. The C1s signal peak appeared at approximately 284.8 eV, corresponding to an atmospheric contamination or carbon formed throughout upon calcination.

The peaks of the three constituent elements of the ZVO such as: Zn (Zn2p), V (V2p), and O (O1s) appeared at 1021.4, 517.2, and 530.2 eV, respectively. Fig. 2b shows the high-resolution Zn 2p spectrum. Thus, the binding energy peaks at 1021.5 and 1044.6 eV could reasonably be attributed to Zn 2p3/2 and Zn 2p1/2 of Zn^{2+}, respectively[68]. The binding energy peaks located at approximately 525.9 and 518.2 eV (Fig. 2C) were the result of the spin-orbit doublets V 2p1/2 and V 2p3/2, respectively. These peak positions are characteristic of the presence of V^{5+} ions[69]. In addition, the high-resolution O1s spectrum could be resolved into three components

at 530.8, 531.7, and 533.3 eV (Fig. 2c). The first and second peaks can be assigned to the lattice oxygen since oxygen has two different local environments (O-Zn and O-V). The peak at 533.3 eV was due to the adsorbed oxygen. However, it is highly probable that there is an electronic dynamic exchange between zinc and vanadium, which underlies the exceptional catalytic performance of ZVO. It has been shown that the acid and base contents of the catalysts determine their catalytic activities[70]. The acid strength of the ZVO was also measured using the TPD method based on the various desorption temperatures of NH_3 on acid sites. A broadband in the NH_3-TPD-curve was observed, which could be separated into several well distinguishable maxima over a temperature range from 100 to 650 °C (Fig. 3). The amounts of desorbed NH_3 at different temperatures were calculated based on the relative areas of the corresponding bands of desorbed NH_3 using the following equation:

$$Q = Q_n \times A/A_T \times 100\%$$

Where Q_n (mmol/g) is the total amount of desorbed-NH_3, A is the corresponding area of a givenNH_3-desorption peak, A_T is the total area of all of the NH_3-desorption peaks, and Q (mmol/g) is the amount of desorbed NH_3 corresponding to the TPD peak of relative area A. Various bands appeared due to the signals of NH_3-physisorption on the ZVO surface at low temperatures (≤150 °C), and NH_3-chemisorption on acid sites at higher temperatures. Small strips appeared at around 180 and 209 °C, corresponding to Lewis acid centers that were generated from bivalent Zn^{2+} and pentavalent V^{+5}[71]. In addition, it should be noted that the surface –OH groups represent Brønsted acidity[32, 72], which depend on the atomic arrangement in the crystalline three-dimensional lattice and the nature of chemical bonds between atoms.

We note that the highest acid content appeared in the ZVO after heating above200 °C. Various acid sites were detected as medium, strong, and very strong at desorption temperatures of approximately 209, 256, 316, 412, and 550 °C, respectively. The largest amount of medium- and strong-strength acid sites appeared at 209 °C (0.0032 mmol/g), at 256 °C (0.012 mmol/g),

and at 316 °C (0.0061 mmol/g). Moreover, the very strong-strength acid sites were more abundant at412 °C (0.01 mmol/g) than at550 °C (0.0011 mmol/g). This variety of acid sites should be beneficial for catalytic reactions [73].Thus, we conclude that only medium- and strong-strength acid sites existed in the ZVO, with a predominance of both types of sites. This can be explained by the complex geometry of the ZVO surface since it is a mixed oxide, and also due inter-facial zones, which play a key role in the sorption phenomena in heterogeneous media.

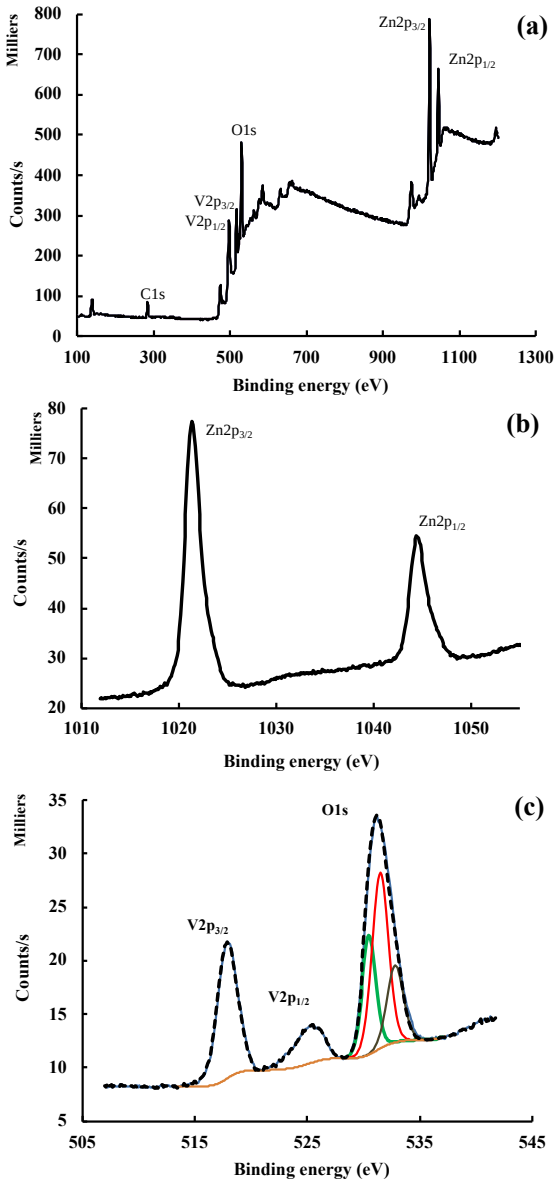

Figure 2: XPS spectra: (a) survey spectrum, (b) Zn2p, (c) V2p and O1s.

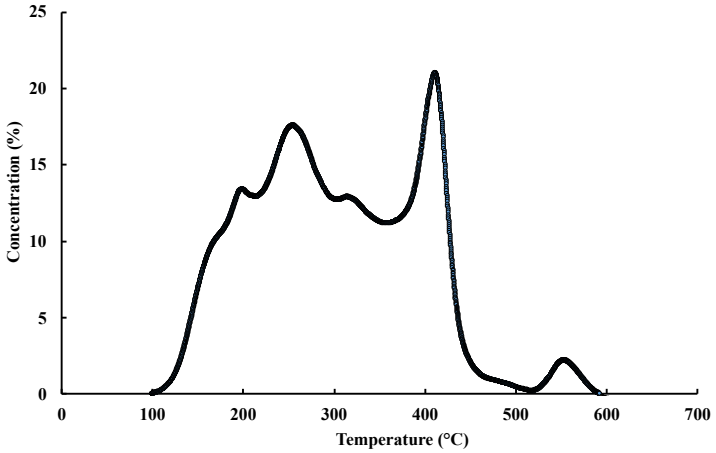

Figure 3: NH_3-TPD curve of the ZVO

Table 2. Codified and experimental values of the runs performed in the experimental design corresponding to glucose oxidation

Runnumber (RN)	H_2O_2 (mmol) X1	Power (W) X2	Temperature (°C) X3	Time (min) X4	$Y_{Glucose}$: conversion glucose		Selectivity (%)										
					Experimental	Predicted	OA1	OA2	OA3	OA4	OA5	OA6	OA7	OA8	OA9	OA10	HMF
1	0.012	200	100	5	15.2	11.4	---	1.1	---	---	---	---	---	---	---	---	---
2	0.2	200	100	30	88.2	87.5	1.9	5.1	35.2	8.0	14.5	5.3	2.8	2.6	1.0	---	---
3	0.2	800	50	5	16.2	11.0	---	0.5	---	---	---	1.3	---	---	---	---	---
4	0.2	600	100	30	100	99.5	2.0	6.2	59.8	7.0	12.5	1.5	1.0	1.6	1.2	---	---
5	0.2	800	100	17.5	68.3	69.6	---	12.6	1.6	1.2	3.8	2.6	---	---	0.6	2.3	0.2
6	0.012	800	100	30	94.3	95.1	10.3	0.2	25.3	8.0	7.6	12.8	2.8	5.0	6.8	---	0.6
7	0.106	600	75	17.5	64.3	66.2	12.2	7.2	1.8	9.0	3.1	---	1.7	12.5	---	---	0.9
8	0.2	200	75	5	22.3	23.2	---	5.3	---	---	---	---	---	---	---	---	---
9	0.106	600	75	17.5	66.1	65.7	12.4	7.2	1.9	9.0	3.1	---	1.5	12.2	---	---	0.8
10	0.106	600	75	5	23.1	25.7	---	10.0	2.3	---	---	---	---	---	---	---	---
11	0.012	600	100	17.5	56.2	57.7	15.8	---	12.3	6.5	8.9	---	13.8	---	---	---	0.1
12	0.012	200	75	30	80.3	85.3	1.3	8.5	24.3	11.3	16.2	---	5.6	2.8	---	---	1.8
13	0.106	600	75	17.5	69.2	65.7	12.3	7.8	1.9	8.8	2.9	-	1.6	12.0	---	---	1.0
14	0.012	600	50	30	61.2	61.8	14.2	1.8	5.6	5.8	---	10.2	---	---	---	---	---
15	0.106	200	75	17.5	67.3	60.7	1.3	2.3	3.8	5.8	5.6	1.6	2.8	---	---	---	---
16	0.012	200	50	5	12	10.3	---	1.8	---	---	3.5	---	---	---	---	---	---
17	0.106	800	50	17.5	39.8	42.7	12.3	---	---	---	---	---	10.6	---	---	2.8	---
18	0.012	800	75	5	12.2	11.8	2.4	0.6	---	---	---	---	---	---	---	---	---
19	0.2	200	50	30	42.2	44.5	---	2.3	7.8	---	---	3.5	12.8	5.3	4.0	---	---
20	0.106	800	100	5	15.8	10.3	0.8	---	---	---	4.3	---	---	---	---	---	---
21	0.2	800	75	30	98.8	98.8	5.8	8.3	35.3	5.2	11.1	6.7	3.8	---	---	---	2.3

OA1: Oxalicacid, OA2: Glucuronicacid, OA3: Galacturonicacid, OA4: Malicacid, OA5: Malonicacid, OA6: Succinicacid, OA7: Lacticacid, OA8: Formicacid, OA9: Aceticacid, OA10: Levulinicacid, OA11: Glycolicacid, HMF: Hydroxymethylfurfural

3.2. Experimental design, analysis, optimization, and catalytic testing results

Optimization of the oxidation of sugars by the ZVO was performed using a Box-Behnken design. Several variables that could potentially affect the efficiency of this catalytic process were chosen, such as: the H_2O_2concentration (mmol), microwave power (W), temperature (°C), and time (min). The other parameters in this chemical process were kept constant, such as the solvent volume and the ratio of the amount of sugar vs. catalyst. The results provided a statistical model, which was used to identify high conversion and selectivity trends for the catalytic process. The equations below illustrate the relationship of the aforementioned

variables. The coefficients of the model developed in Eq.1 were estimated by multiple regression analysis.

Eq.1

$$Y_{conversion} = \beta_0 + \sum_{i=1}^{4} \beta_i X_i + \sum_{i=1}^{4} \beta_{ii} X_i^2 + \sum \sum_{i<j=1}^{4} \beta_{ij} X_i X_j$$

Where $Y_{conversion}$is the predicted response variable; X_i. X_j(i=1. 4; j=1. 4; i#j) represent the coded independent variables (microwave conditions); β_0 is the intercept coefficient; $\beta_i$are the linear terms; β_{ii} are the squared terms; and $\beta_{ij}$are the interaction terms. The polynomial models for the sugars (xylose and glucose conversion; Y(xylose or glucose)) are presented in Eq. 2 and Eq.3, respectively:

Eq. 2

$$Y_{Xylose\ conv} = 66.58 + 1.75X_1 + 2.49X_2 + 9.83X_3 + 33.38X_4 + 4.21X_1X_2 + 1.33X_1X_3 - 1.87X_1X_4 + 4.55X_2X_4 - 0.23X_2X_3 + 8.04X_3X_4 - 2.51X_1^2 - 2.39X_2^2 - 13.05X_3^2 - 5.97X_4^2$$

Eq. 3

$$EY_{Glucose\ conv} = 65.65 + 2.28X_1 + 2.46X_2 + 10.61X_3 + 33.68X_4 + 3.95X_1X_2 + 1.98X_1X_3 - 1.58X_1X_4 + 4.34X_2X_4 - 0.41X_2X_3 + 8.50X_3X_4 - 1.71X_1^2 - 2.49X_2^2 - 12.68X_3^2 - 6.30X_4^2$$

Table 3: Codified and experimental values of the runs performed in the experimental design corresponding to xylose oxidation

Runnumber (RN)	H_2O_2 (mmol) X1	Power (W) X2	Temperature (°C) X3	Time (min) X4	Y_{xylose}: conversion xylose		Selectivity (%)								
					Experimental	Predicted	OA1	OA4	OA5	OA6	OA7	OA8	OA9	OA11	Furfural
1	0.012	200	100	5	16.2	12.4	0.01	---	---	---	---	1.2	---	---	---
2	0.2	200	100	30	84.2	83.9	---	0.1	---	---	2.0	30.3	6.8	34.5	---
3	0.2	800	50	5	13.2	12.0	---	---	---	---	---	3.0	---	---	---
4	0.2	600	100	30	100	98.8	4.2	---	0.5	2.3	---	8.0	30.2	39.8	3.5
5	0.2	800	100	17.5	67.3	68.2	12.6	1.0	---	---	5.0	9.6	---	15.3	---
6	0.012	800	100	30	96.3	95.5	0.5	1.3	---	2.8	1.3	8.3	39.2	29.5	---
7	0.106	600	75	17.5	70.3	65.8	4.2	---	---	3.9	---	10.0	25.0	17.1	---
8	0.2	200	75	5	23.3	23.8	3.0	1.05	---	---	---	---	---	4.1	---
9	0.106	600	75	17.5	71.1	69.6	1.1	---	5.8	8.9	6.8	4.8	10.1	15.8	0.5
10	0.106	600	75	5	26.2	27.2	---	---	0.3	1.2	---	---	---	3.0	---
11	0.012	600	100	17.5	58.5	57.8	10.5	---	0.9	3.5	---	12.5	1.12	15.6	0.1
12	0.012	200	75	30	81.3	86.4	5.0	---	10.3	2.8	8.7	10.3	20.2	14.8	1.3
13	0.106	600	75	17.5	70.2	66.6	4.3	---	---	3.8	---	9.8	25.3	17.3	---
14	0.012	600	50	30	63.2	62.8	---	1.3	15.3	---	---	---	20.0	10.5	---
15	0.106	200	75	17.5	68.3	61.7	1.3	---	5.9	8.5	6.9	4.9	11.1	14.8	0.4
16	0.012	200	50	5	13	11.4	---	0.2	0.6	---	---	---	---	---	---
17	0.106	800	50	17.5	44.8	43.8	7.8	---	---	---	---	9.3	-	19.3	---
18	0.012	800	75	5	13.2	12.4	---	---	---	0.05	---	---	1.3	---	---
19	0.2	200	50	30	43.2	45.4	---	15.0	---	9.5	---	14.5	---	---	---
20	0.106	800	100	5	16.6	11.5	0.5	---	---	---	---	2.1	---	---	---
21	0.2	800	75	30	99.8	95.9	2.8	1.2	---	3.0	18.3	14.8	8.8	12.8	---

OA1: Oxalicacid, OA2: Glucuronicacid, OA3: Galacturonicacid, OA4: Malicacid, OA5: Malonicacid, OA6: Succinicacid, OA7: Lacticacid, OA8: Formicacid, OA9: Aceticacid, OA10: Levulinicacid, OA11: Glycolicacid, HMF: Hydroxymethylfurfural

The design matrix comprising 21 experiments for each sugar (xylose and glucose) along with their experimental and predicted responses are shown in Tables 2 and 3. The results show a high level of concordance between the experimental and the predicted responses. The degree

of conversion was found to range from 11 to 100%. The fit quality of the sugar (glucose and xylose) conversion model was confirmed with analysis of variance (ANOVA)[74]. It should be noted that the ANOVA analysis was required to justify the significance and adequacy of the model. The value of (Prob>F) was used as a tool to check the significance of each of the model's terms. Significance of the corresponding model terms involves having a higher Fisher's value (F-value) with a probability (p-value) that is as low as possible ($p<0.05$)[75]. Table 4 shows the analysis of variance (F-test) and the p-value for this experiment. The p-value of the model was 0.002, which indicates that the model was acceptable for use in this experiment.

Table 4: Analysis of variance (ANOVA) for the fitted quadric polynomial model for optimization of sugar conversion under microwave conditions

Source	D.F		Sum of Squares		Mean Square		F-value
	Xylose	Glucose	Xylose	Glucose	Xylose	Glucose	Xylose
Model	14	14	19,254.938	19,972.852	1,375.35	1,426.63	13.6544
Residual	6	6	544.7	620.137	90.8	103.36	---
C. Total	20	20	19,859.291	20,592.99	---	---	---
R^2= 0.97; Adj. R^2= 0.96							

The calculated F-value for the regression was more than 13.6, which is much higher than the value from the Fisher tables ($F_{14.6}$ =3.9, for a 95% confidence level), confirming that the model is a good fit of the experimental data[76, 77]. The determination coefficient R2 =0.97 implies a reasonable fit between the experimental and the predicted values[78]. It allows it to be inferred that 97% of the total variation in the response is justified by the fitted model. The adjusted R2 (Adj R2) is also a measure of how good the fit is[79]. It changes the value of R2 by taking into account the number of covariates or predictors in the model. In this case Adj R2 (0.96) was very close to the R2 value. The regression coefficients of Eq. 2/Eq. 3 and the corresponding p-values are presented in Table 5. These results indicate that the linear effects of time (X4) and temperature (X3) were the principal determining factors for the response on sugars conversion. X3X4 (Temperature*Time) was chosen as the interaction key for the response surface and contour plots presented in Figure 4,asit has a low p-value compared to the other interactions that are not significant due to a p-value greater than 0.1[80]. Figures 4(a), (b), (c), and (d) depict

the 3D surface responses and contour plots of the conversions of xylose and glucose as a function of time and temperature.

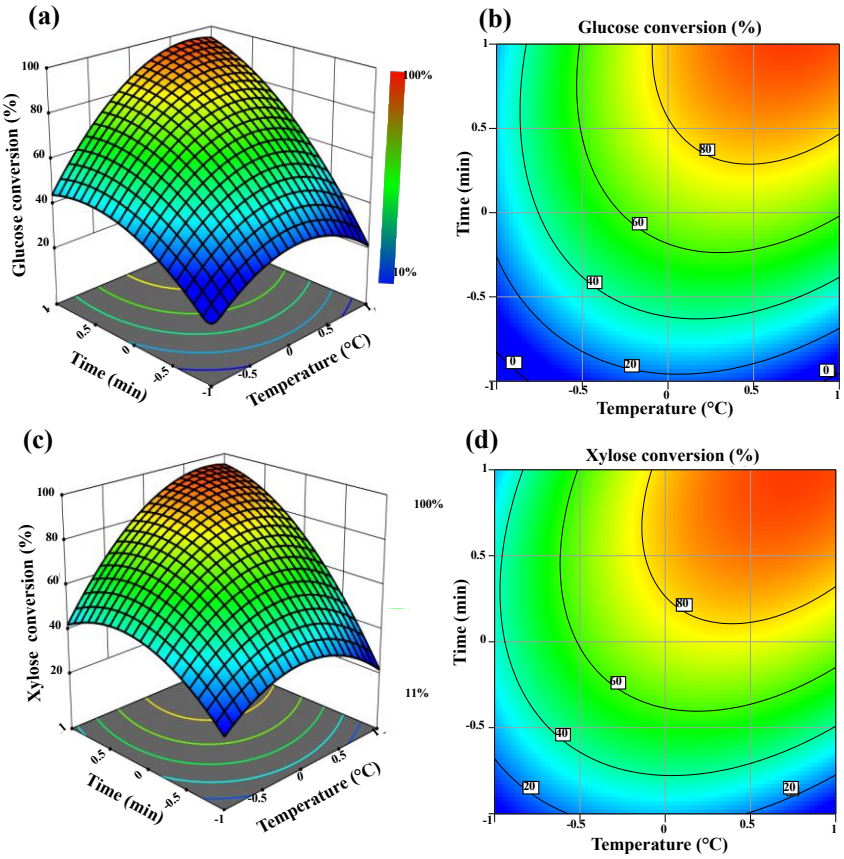

Figure 4: 3D response surface and contour plots of sugar conversion for different coded values of temperature (°C) and time (min): glucose (a) & (b); xylose (c) & (d)

Table 5: Estimated regression coefficients and corresponding p-values obtained with Box-Behnken designs for sugar conversions

Parameter	Term	Estimate		Std Error		t-value		p-value	
		Xylose	Glucose	Xylose	Glucose	Xylose	Glucose	Xylose	Glucose
β_0	Intercept	66.58	65.66	4.95	5.01	13.45	13.10	<.0001	<.0001
β_1	X1	1.75	2.23	2.88	2.92	0.61	0.76	0.5654	0.4745
β_2	X2	2.49	2.46	2.83	2.86	0.88	0.86	0.4116	0.4228
β_3	X3	9.84	10.61	3.06	3.10	3.22	3.42	0.0182	0.0141
β_4	X4	33.38	33.68	2.88	2.92	11.58	11.53	<.0001	<.0001
β_{11}	X1*X1	-2.51	-1.70	5.40	5.47	-0.46	-0.31	0.6586	0.7661
β_{12}	X1*X2	4.22	3.95	3.19	3.23	1.32	1.22	0.2345	0.2670
β_{22}	X2*X2	-2.40	-2.49	5.73	5.81	-0.42	-0.43	0.6904	0.6830
β_{13}	X1*X3	1.33	1.98	3.49	3.54	0.38	0.56	0.7162	0.5963
β_{23}	X2*X3	-0.02	-0.40	3.43	3.48	-0.01	-0.12	0.9947	0.9114
β_{33}	X3*X3	-13.05	-12.68	4.84	4.90	-2.70	-2.59	0.0357	0.0414
β_{14}	X1*X4	-1.88	-1.58	3.24	3.28	-0.58	-0.48	0.5832	0.6463
β_{24}	X2*X4	4.56	4.35	3.19	3.23	1.43	1.34	0.2032	0.2272
β_{34}	X3*X4	8.04	8.50	3.49	3.54	2.30	2.40	0.0609	0.0532
β_{44}	X4*X4	-5.97	-6.30	5.40	5.47	-1.11	-1.15	0.3113	0.2935

Conversion is enhanced as the residence time and the temperature increase. The combined effect of the two factors was positive and statistically significant, as also revealed by the contour plots and Table 5. The optimum conditions for maximum conversion of the sugars (xylose/glucose) into organic acids were: H_2O_2=0.207 mmol, power=500 W, temperature=100 °C, and time=30 min. The temperature and the microwave power profile vs. time is presented in **Fig S5**. Both of the sugars were converted quantitatively. The optimized results of conversion under these conditions gave rise to a total conversion of 97.3% (0.17% difference with the theoretical value). Tables2 and 3 summarize the oxidation conversions for xylose and glucose and also the selectivity into each organic acid obtained by this catalytic process. It should be noted that the selectivity of the glucose and xylose oxidation reactions depends on the experimental conditions (Tables2 and 3). For example, the oxidation of glucose in the presence of 0.012 mmol of H_2O_2 at 100 °C for 5 min, resulted in the production of glucuronic acid only, with a conversion of 15.2% and a selectivity of 1.1% (Table 2, RN-1). It was also noted that all of the reactions lasting 5 minutes resulted in a maximum of two acids, with a conversion of no more than 22% (Table 2: RN-3, RN-8, RN-10, RN-16, RN-18, and RN-20). This was independent of the other glucose oxidation parameters. An increase of certain reaction parameters allowed for enhancement of the conversion of the substrate (glucose)by oxidation. However, the selectivity was not absolute. For example, prolongation of the reaction time, as well as an increase in temperature, revealed that the conversion was quantitative with varying selectivities. Generally, the longer the reaction time the more the conversion went to completion. On the other hand, the selectivity was sensitive to the amount of H_2O_2. The influence of microwave power appeared to be due to a rise in temperature (known as the 'magical effect' of microwaves). These parameters can be optimized by judicious choice of the two parameters: time and temperature, and by using a fixed amount of H_2O_2. Thus, analysis of the RN-4 reaction mixture (Table 2) showed that the conversion was complete with the formation of a product mixture, indicating excellent selectivity of approximately 59.8% to

galacturonic acid. Table 2 also shows the selectivity of the products obtained during oxidation of xylose on the ZVO. For tests lasting 5 min, the reactions led to very weak conversions and with selectivities in two to three acids that were detected in quantities that remained limited and variable based on the other parameters (RN-1, RN-3, RN-1, RN-8, RN-10, RN-16, RN-18, and RN-20). For example, (RN-8, 23.3% conversion), the oxidation gave rise to a selectivity of 4.1% into glycolic acid and 1.05% into malic acid. The conversions were systematically more substantial when the reaction time was extended to 30 min, but also with an increase of the temperature to 100 °C. At 100% conversion, acetic acid and glycolic acid were present in larger amounts: 30.2% and 39.8%, respectively (Table 2, RN-4). The selectivities in majority products, obtained as a function of the reaction time, are presented for tests RN-4 and RN-5 (Table 3) with two different powers, with the same temperature and the same amount of H_2O_2. The oxidation time appears to have a significant effect on the conversion and selectivity. On the other hand, the selectivity of oxidation into glycolic acid decreased to 29.5% and the selectivity of oxidation into acetic acid increased to 39.2% when we used a small amount of H_2O_2 (0.012 mmol), although the other parameters remained constant (Table 3, RN-6). For the two organic acids (acetic acid and glycolic acid), the selectivities were moderately affected by the changes in the key parameters of this catalytic process. On the other hand, the selectivities into other organic acids remained mostly low compared with acetic acid and glycolic acid. These observations confirm that the increase in temperature and the prolongation of xylose oxidation had a beneficial effect on the conversion rate and also on the selectivity of the oxidation into those two acids (acetic acid and glycolic acid). After having optimized the parameters of the oxidation of the two sugars via the experimental design and then experimental validation of these optimized conditions, we adopted these parameters (H_2O_2 = 0.207 mmol, power = 500 W, temperature = 100 °C, and time = 30 min)to oxidize glucose and xylose, respectively. We thereby obtained a total (100%) conversion of glucose, with preferential formation of galacturonic acid (Table 6).

Table 6 Selective oxidation of glucose and xylose by H_2O_2 over ZVO under microwave irradiation[a]

Substrate	Conversion (%)	Selectivity (%)									
		Glucuronic acid	Galacturonic acid	Malic acid	Succinic acid	Malonic acid	Lactic acid	Glycolic acid	Acetic acid	Oxalic acid	Formic acid
Glucose	100	7.99	**59.62**	7.21	1.52	12.66	1.04	---	1.29	3.63	1.66
Xylose	100	---	---	0.49	0.21	---	2.39	**46.26**	**39.19**	2.21	7.84

[a] Reaction conditions: 100 mg of sugar was dissolved in water and in the presence of H_2O_2, with a total volume (10 mL), after which 10 mg of the ZVO was added. The reaction mixture was then transferred to a Teflon-sealed MW reactor and exposed to MW irradiation (500 W), at 100 °C for30 min. After cooling to room temperature, the catalyst was separated by centrifugation and the final mixture was analyzed by HPLC.

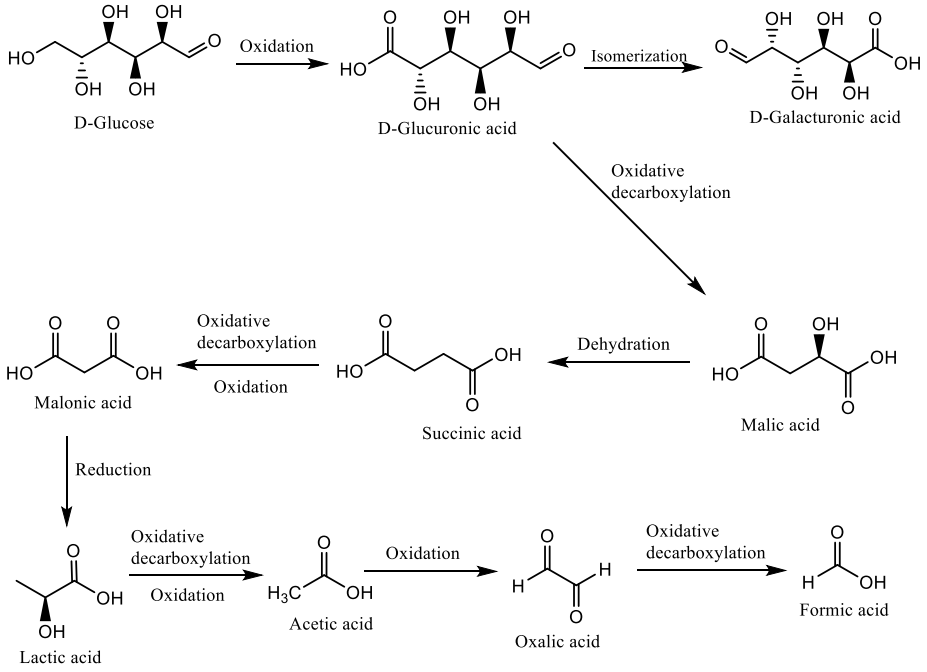

Scheme 1: Proposed selective oxidation of glucose to galacturonic acid

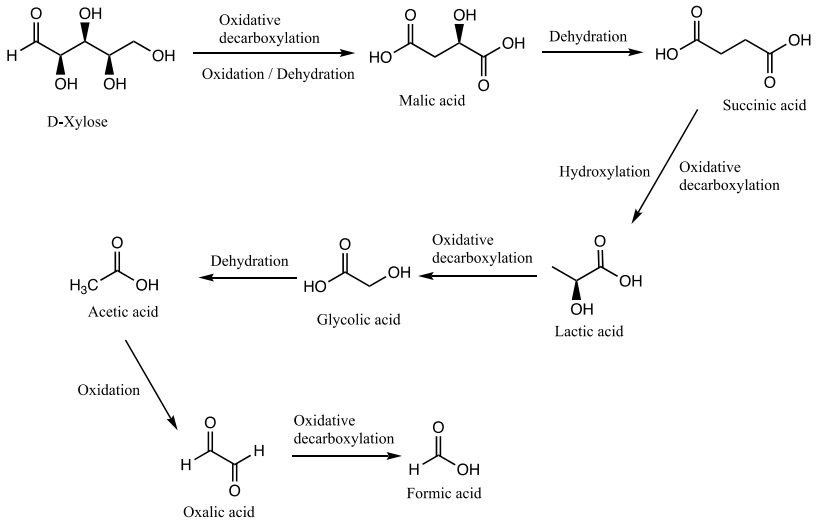

Scheme 2: Proposed selective oxidation of xylose to glycolic acid

This shows that this catalytic process was exclusively selective into this acid (59.62%). The other acids formed were obtained with low and variable selectivities: 7.99% into glucuronic

acid, 7.21% into malic acid, 1.52% into succinic acid, 12.66% into malonic acid, 1.04% into lactic acid, 1.29% into acetic acid, 3.63% into oxalic acid, and 1.66% into formic acid (Table 6).. This catalytic process gave rise initially to two conformational isomers: galacturonic acid and glucuronic acid. It should be noted that galacturonic acid is the most stable isomer; which means it is less reactive. Glucuronic acid is the least stable conformational isomer (more reactive). The rest of this process was a succession of reactions from glucuronic acid (Scheme 1). In the case of xylose, the conversion was also complete under the optimized conditions (Table 6). We thereby obtained a mixture of organic acids namely: malic acid, succinic acid, lactic acid, glycolic acid, acetic acid, oxalic acid, and formic acid. Oxidation of xylose under these conditions selectively yielded: glycolic acid (46.26%) and acetic acid (39.19%). The other acids were obtained with very low selectivities. Scheme 2 summarizes the progress route of the reaction, which is a sequence of reactions. Glucose oxidation was considerably accelerated and also more selective in favor of galacturonic acid, in water under microwave irradiation and over the ZVO. Similarly, the xylose oxidation revealed the catalytic performance of the ZVO under optimized conditions. The origin of this acceleration and increased selectivity can be attributed to: (i) the presence of a large amount of acid sites on the ZVO, which has both Lewis acidity and a particular pronounced Brønsted acidity, (ii) the hydrophilic effect of the reactants with water (reaction solvent) since the sugars are homogeneously dissolved in the water, which can minimize adverse interactions between the reagents (sugar/oxidant: H_2O_2) and the solvent by creating hydrogen bonds (*reaction 'in-water*')[81], and (iii) the microwave effect, which can promote these types of reactions. Basically, the selectivity of the reaction can be affected, on the one hand, by the experimental conditions, and, on the other hand, by the nature of the catalyst. The catalytic performance of the ZVO is detailed in Table . In summary, the efficiency of this catalytic system and the reaction conditions ("*Chimie douce"*) make this process a powerful synthetic tool capable of producing organic acids with high selectivity to form a wide range of high value-added molecules.

These results reveal that zinc vanadium mixed oxide synthesized by co-precipitation has significant catalytic activity in the oxidation of glucose and xylose in terms of the reaction time and the degree of conversion compared to previous studies[82,83,84]

3.3. Catalyst regeneration and performance

As testing regeneration is essential in this type of study, we have assessed the feasibility of reusing the ZVO for three run-cycles to validate this concept, and we studied its stability. A simple procedure based on washing and drying was developed to restore this catalyst to its initial activity. Using the same reaction conditions, we tested the recovered ZVO after washing and drying it. Figures 5 & 6 present the selectivity distribution of the principal organic acids obtained as a function of the run. It can be seen that the same selectivities were obtained for each run-cycle. Thus, the ability to selectively convert glucose to galacturonic acid remained unchanged. Similarly, the oxidation of xylose follows the same reaction route, thus favoring the same selectivity being obtained after three run-cycles of reuse. These observations confirm that the reuse of the ZVO in three cycles did not have a deactivating effect on its catalytic performance, which remained stable under the reaction conditions.

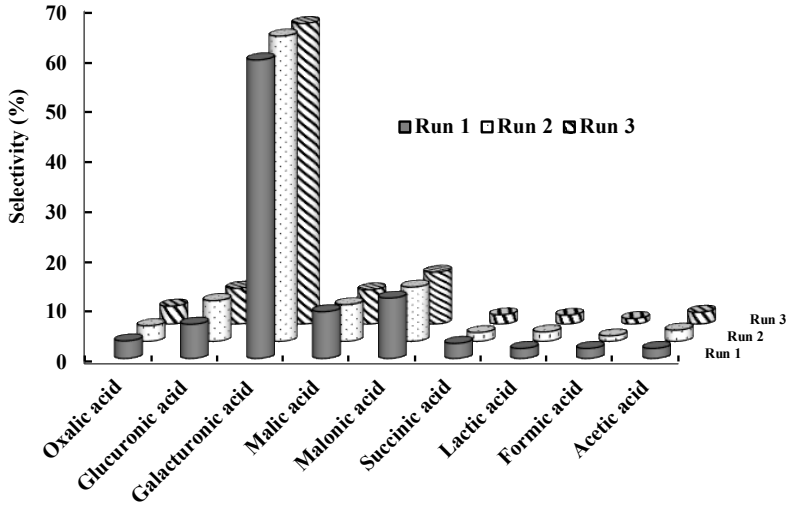

Figure 5: ZVO recycling and selective oxidation of glucose under the optimized conditions.

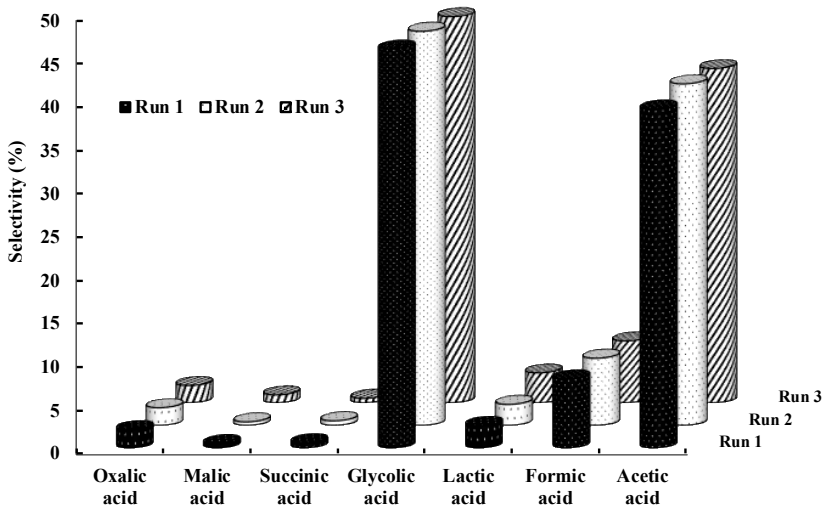

Figure 6: ZVO recycling and selective oxidation of xylose under the optimized conditions.

Thus, this catalytic system behaved robustly and the original strong-acid character was retained during the regeneration tests. From an analytical point of view, the ZVO recovered from the glucose oxidation reaction remained mechanically stable since the XRD revealed no change in its crystalline structure (Fig. S2 (b)). Similarly, using SEM, we noted that the ZVO surface remained unchanged (Fig. S6). XPS analysis was further used to determine the chemical composition and the oxidation state of the recovered sample after it was washed and dried. As shown in Fig. S7, the survey spectrum, the high-resolution spectra of V2p and Zn2p, further confirm that this recovered sample retained its initial characteristics (electronic structure and oxidation state). With the exception of two points: (i) the intensity of the carbon peak, which became larger compared to the peak in the spectrum of freshly prepared ZVO, thus revealing contamination resulting from non-significant sugar since the ZVO retained its catalytic performance, and (ii) the appearance of four peaks of oxygen at 530.3, 531.3, 532.5, and 534.1 eV (Fig. 7), which correspond to the lattice oxygen, the adsorbed-oxygen during growth of the ZVO, and adsorption of the oxygen resulting from the decomposition of H_2O_2.

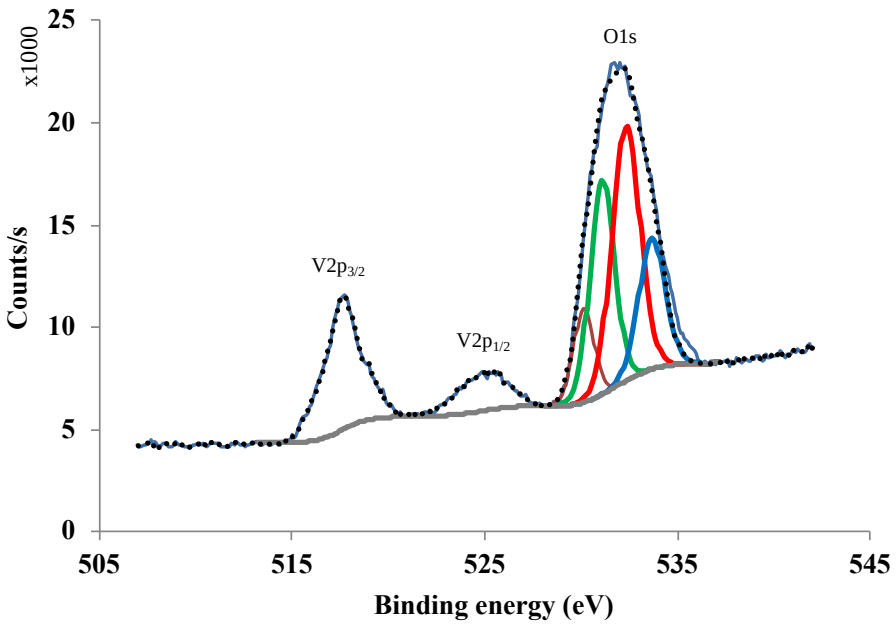

Figure 7: High-resolution spectra of the recovered ZVO: 2p and O 1s.

4. Conclusion

In summary, the work presented here was aimed at exploring a new paradigm for glucose and xylose selective oxidation to galacturonic acid and glycolic acid, respectively by a ZVO catalyst under microwave irradiation. The ZVO was obtained by a straight forward precipitation method, and it was examined using several characterization tools. Response surface methodology (RSM) was applied to find the optimal operating conditions in order to maximize the sugar conversion and to improve the oxidation selectivity. Based on the model prediction, the optimum conditions for sugar oxidation over ZVO under microwave irradiation were: H_2O_2=0.207 mmol, power= 500 W, temperature=100 °C, and time=30 min, with a total level of conversion of 97.3%. By adopting these optimized parameters, in the case of glucose oxidation, we obtained galacturonic acid with a selectivity of 59.62%, and total (100%)conversion. In the case of oxidation of xylose, we obtained glycolic acid with a selectivity of 46.26% and acetic acid with a selectivity of 39.19%. This shows that these reactions were selective under these conditions using the ZVO as a catalyst.

Acknowledgments

This work was sponsored by the INRA-SupAgro at Montpellier in France, and also by the Mohammed VI Polytechnic University (UM6P) at Benguerir in Morocco. We thank the technical support of the OpenMind and LipPolGreen platform of the UMR IATE at Montpellier for their support.

References

[1] H. Yong Lee, A. Rong Kim, M. Park, J. Min Jo, D. Hyun Lee, J. Wook Be, Combined steam and CO2 reforming of CH4 using coke oven gas onnickel-based catalyst: Effects of organic acids to nickel dispersionand activity, Chemical Engineering. 280 (2015) 771 781.

[2] C. Perego, D. Bianchi, Biomass upgrading through achid-base catalysis, Chemical engineering journal. 161 (2010) 314-322.

[3] H. Quitmann, R. Fan, P. Czermak, Acidic Organic Compounds in Beverage, Food, and Feed Production, in: H. Zorn, P. Czermak (Eds.) Biotechnology of Food and Feed Additives, Springer-Verlag Berlin, Berlin. (2014) 91-141.

[4] W. Deng, Y. Wang, N. Yan, Production of organic acids from biomass resources, Current Opinion in Green and Sustainable Chemistry. 2 (2016) 54-58.

[5] P. Rogers∗ , J.-S. Chen, M.J. Zidwick, Organic Acid and Solvent Production: Acetic, Lactic, Gluconic, Succinic, and Polyhydroxyalkanoic Acids, in: E. Rosenberg, E.F. DeLong, S. Lory, E. Stackebrandt, F. Thompson (Eds.) The Prokaryotes: Applied Bacteriology and Biotechnology, Springer Berlin Heidelberg, Berlin, Heidelberg. (2013)3-75.

[6] P. Pal, R. Kumar, S. Banerjee, Manufacture of gluconic acid: A review towards process intensification for green production, Chemical Engineering and Processing: Process Intensification, 104 (2016) 160-171.

[7] A.M. Cañete-Rodríguez, I.M. Santos-Dueñas, J.E. Jiménez-Hornero, A. Ehrenreich, W. Liebl, I. García-García, Gluconic acid: Properties, production methods and applications—An excellent opportunity for agro-industrial by-products and waste bio-valorization, Process Biochemistry. 51 (2016) 1891-1903.

[8] T.H. Emaga, N. Rabetafika, C.S. Blecker, M. Paquot, Kinetics of the hydrolysis of polysaccharide galacturonic acid and neutral sugars chains from flaxseed mucilage, Biotechnologie Agronomie Societe Et Environnement, 16 (2012) 139-147.

[9] C. Blecker, S. Danthine, M. Petre, G. Lognay, B. Moreau, L.V. Elst, M. Paquot, C. Deroanne, Enzymatically prepared n-alkyl esters of glucuronic acid: The effect of freeze-drying conditions and hydrophobic chain length on thermal behavior, Journal of Colloid and Interface Science. 321 (2008) 154-158.

[10] N. Ferlin, D. Grassi, C. Ojeda, M.J.L. Castro, E. Grand, A.F. Cirelli, J. Kovensky, Synthesis of sugar-based chelating surfactants for metal removal from wastewater, Carbohydr. Res. 343 (2008) 839-847.

[11] A. Richel, F. Nicks, P. Laurent, B. Wathelet, J.-P. Wathelet, M. Paquot, Efficient microwave-promoted synthesis of glucuronic and galacturonic acid derivatives using sulfuric acid impregnated on silica, Green Chemistry Letters and Reviews. 5 (2012) 179-186.

[12] T. Mahrholz, J. Klein, T. Klein, New poly(sodium carboxylate)s based on saccharides, 1 - Synthesis and characterization of ionic allyl glycoside polymers, Macromol. Chem. Phys. 203 (2002) 2640-2649.

[13] D. Doyle, P.V. Murphy, Synthesis of novel glycophanes derived from glucuronic acid by ring closing alkene and alkyne metathesis, Carbohydr. Res., 343 (2008) 2535-2544.

[14] V.A. Timoshchuk, Uronic acids: synthesis and reactions, Russian chemical reviews. 64 (1995) 721-750.

[15] R.C. Sun, J.M. Lawther, W.B. Banks, Fractional and structural characterization of wheat straw hemicelluloses, Carbohydrate Polymers. 29 (1996) 325-331.
[16] K.B.H. Finch, R.M. Richards, A. Richel, A.V. Medvedovici, N.G. Gheorghe, M. Verziu, S.M. Coman, V.I. Parvulescu, Catalytic hydroprocessing of lignin under thermal and ultrasound conditions, Catalysis Today. 196 (2012) 3-10.
[17] S. Veeravali, A P. Mathews, Continuous fermentation of xylose to short chain fatty acids by Lactobacillusbuchneri under low pH conditions, Chemical Engineering journal. 337 (2018) 764-771
[18] A.M. Cañete-Rodríguez, I.M. Santos-Dueñas, M.J. Torija-Martínez, A. Mas, J.E. Jiménez-Hornero, I. García-García, Preparation of a pure inoculum of acetic acid bacteria for the selective conversion of glucose in strawberry purée into gluconic acid, Food and Bioproducts Processing. 96 (2015) 35-42.
[19] H. Zhang, G. Liu, J. Zhang, J. Bao, Fermentative production of high titer gluconic and xylonic acids from corn stover feedstock by Gluconobacter oxydans and techno-economic analysis, Bioresource Technology. 219 (2016) 123-131.
[20] W. Deng, Q. Zhang, Y. Wang, Catalytic transformations of cellulose and cellulose-derived carbohydrates into organic acids, Catalysis Today. 234 (2014) 31-41.
[21] Z. Zhang, G.W. Huber, Catalytic oxidation of carbohydrates into organic acids and furan chemicals, Chemical Society Reviews. 47 (2018) 1351-1390.
[22] H. Li, P.S. Bhadury, A. Riisager, S. Yang, One-pot transformation of polysaccharides via multi-catalytic processes, Catalysis Science & Technology. 4 (2014) 4138-4168.
[23] H. Li, X. Kong, Z. Fang, R. L. Smith, Chapter 1 Fundamentals of Bifunctional Catalysisfor Transforming Biomass-RelatedCompounds into Chemicals and Biofuels, Biofuels and Biorefineries. 8 (2017).,
[24] D. Chen, F. Liang, D. Feng, M. Xian, H. Zhang, H. Liu, F. Du, An efficient route from reproducible glucose to 5-hydroxymethylfurfuralcatalyzed by porous coordination polymer heterogeneous catalysts, Chemical Engineering Journal. 300 (2016) 177-184.
[25] M. Besson, P. Gallezot, C. Pinel, Conversion of Biomass into Chemicals over Metal Catalysts, Chemical Reviews. 114 (2014) 1827-1870.
[26] X. Zhang, K. Wilson, A.F. Lee, Heterogeneously Catalyzed Hydrothermal Processing of C5–C6 Sugars, Chemical Reviews. 116 (2016) 12328-12368.
[27] D. Bin, H. Wang, J. Li, H. Wang, Z. Yin, J. Kang, B. He, Z. Li, Controllable oxidation of glucose to gluconic acid and glucaric acid using an electrocatalytic reactor, Electrochimica Acta. 130 (2014) 170-178.
[28] A.T. Governo, L. Proença, P. Parpot, M.I.S. Lopes, I.T.E. Fonseca, Electro-oxidation of d-xylose on platinum and gold electrodes in alkaline medium, Electrochimica Acta. 49 (2004) 1535-1545.
[29] J. Payormhorm, S. Chuangchote, K. Kiatkittipong, S. Chiarakorn, N. Laosiripojana, Xylitol and gluconic acid productions via photocatalytic-glucose conversion using TiO2 fabricated by surfactant-assisted techniques: Effects of structural and textural properties, Materials Chemistry and Physics. 196 (2017) 29-36.
[30] M. Bellardita, E.I. García-López, G. Marcì, B. Megna, F.R. Pomilla, L. Palmisano, Photocatalytic conversion of glucose in aqueous suspensions of heteropolyacid–TiO2 composites, RSC Advances. 5 (2015) 59037-59047.
[31].
[32] D. Gupta, S. Kundu, B. Saha, Efficient dual acidic carbo-catalyst for one-pot conversion of carbohydrates to levulinic acid, RSC Advances. 6 (2016) 100417-100426.
[33] X. Wang, Y. Song, C. Huang, F. Liang, B. Chen, Lactic acid production from glucose over polymer catalysts in aqueous alkaline solution under mild conditions, Green Chemistry. 16 (2014) 4234-4240.

[34] P.N. Amaniampong, Q.T. Trinh, K. Li, S.H. Mushrif, Y. Hao, Y. Yang, Porous structured CuO-CeO2 nanospheres for the direct oxidation of cellobiose and glucose to gluconic acid, Catalysis Today. 306 (2018) 172-182.
[35] T. Lu, Y. Hou, W. Wu, M. Niu, Y. Wang, Formic acid and acetic acid production from corn cob by catalytic oxidation using O2, Fuel Processing Technology. 171 (2018) 133-139.
[36] W. Deng, P. Wang, B. Wang, Y. Wang, L. Yan, Y. Li, Q. Zhang, Z. Cao, Y. Wang, Transformation of cellulose and related carbohydrates into lactic acid with bifunctional Al(iii)–Sn(ii) catalysts, Green Chemistry. 20 (2018) 735-744.
[37] X. Yang, L. Yang, W. Fan, H. Lin, Effect of redox properties of LaCoO3 perovskite catalyst on production of lactic acid from cellulosic biomass, Catalysis Today. 269 (2016) 56-64.
[38] L. Yang, J. Su, S. Carl, J.G. Lynam, X. Yang, H. Lin, Catalytic conversion of hemicellulosic biomass to lactic acid in pH neutral aqueous phase media, Applied Catalysis B: Environmental. 162 (2015) 149-157.
[39] Y. Jiang, L. Yang, C.M. Bohn, G. Li, D. Han, N.S. Mosier, J.T. Miller, H.I. Kenttämaa, M.M. Abu-Omar, Speciation and kinetic study of iron promoted sugar conversion to 5-hydroxymethylfurfural (HMF) and levulinic acid (LA), Organic Chemistry Frontiers. 2 (2015) 1388-1396.
[40] T. Haynes, V. Dubois, S. Hermans, Particle size effect in glucose oxidation with Pd/CB catalysts, Applied Catalysis A: General. 542 (2017) 47-54.
[41] C. Megías-Sayago, J.L. Santos, F. Ammari, M. Chenouf, S. Ivanova, M.A. Centeno, J.A. Odriozola, Influence of gold particle size in Au/C catalysts for base-free oxidation of glucose, Catalysis Today. 306 (2018) 183-190.
[42] A. Abbadi, H. van Bekkum, Effect of pH in the Pt-catalyzed oxidation of d-glucose to d-gluconic acid, Journal of Molecular Catalysis A: Chemical. 97 (1995) 111-118.
[43] Y. Önal, S. Schimpf, P. Claus, Structure sensitivity and kinetics of d-glucose oxidation to d-gluconic acid over carbon-supported gold catalysts, Journal of Catalysis. 223 (2004) 122-133.
[44] M. Comotti, C.D. Pina, M. Rossi, Mono- and bimetallic catalysts for glucose oxidation, Journal of Molecular Catalysis A: Chemical. 251 (2006) 89-92.
[45] A. Onda, T. Ochi, K. Kajiyoshi, K. Yanagisawa, A new chemical process for catalytic conversion of d-glucose into lactic acid and gluconic acid, Applied Catalysis A: General. 343 (2008) 49-54.
[46] J. Lee, B. Saha, D.G. Vlachos, Pt catalysts for efficient aerobic oxidation of glucose to glucaric acid in water, Green Chemistry. 18 (2016) 3815-3822.
[47] K. Morawa Eblagon, M.F.R. Pereira, J.L. Figueiredo, One-pot oxidation of cellobiose to gluconic acid. Unprecedented high selectivity on bifunctional gold catalysts over mesoporous carbon by integrated texture and surface chemistry optimization, Applied Catalysis B: Environmental. 184 (2016) 381-396.
[48] A. Mirescu, U. Prüße, Selective glucose oxidation on gold colloids, Catalysis Communications. 7 (2006) 11-17.
[49] S. Guo, Q. Fang, Z. Li, J. Zhang, J. Zhang, G. Li, Efficient base-free direct oxidation of glucose to gluconic acid over TiO2-supported gold clusters, Nanoscale. 11 (2019) 1326-1334.
[50] C. Megías-Sayago, S. Ivanova, C. López-Cartes, M.A. Centeno, J.A. Odriozola, Gold catalysts screening in base-free aerobic oxidation of glucose to gluconic acid, Catalysis Today. 279 (2017) 148-154.
[51] I. Witońska, M. Frajtak, S. Karski, Selective oxidation of glucose to gluconic acid over Pd–Te supported catalysts, Applied Catalysis A: General. 401 (2011) 73-82.

[52] A.A. Marianou, C.M. Michailof, A. Pineda, E.F. Iliopoulou, K.S. Triantafyllidis, A.A. Lappas, Effect of Lewis and Brønsted acidity on glucose conversion to 5-HMF and lactic acid in aqueous and organic media, Applied Catalysis A: General. 555 (2018) 75-87.
[53] M. Wenkin, R. Touillaux, P. Ruiz, B. Delmon, M. Devillers, Influence of metallic precursors on the properties of carbon-supported bismuth-promoted palladium catalysts for the selective oxidation of glucose to gluconic acid, Applied Catalysis A: General. 148 (1996) 181-199.
[54] R. Wojcieszak, I.M. Cuccovia, M.A. Silva, L.M. Rossi, Selective oxidation of glucose to glucuronic acid by cesium-promoted gold nanoparticle catalyst, Journal of Molecular Catalysis A: Chemical. 422 (2016) 35-42.
[55] P.N. Amaniampong, X. Jia, B. Wang, S.H. Mushrif, A. Borgna, Y. Yang, Catalytic oxidation of cellobiose over TiO2 supported gold-based bimetallic nanoparticles, Catalysis Science & Technology. 5 (2015) 2393-2405.
[56] X. Jin, M. Zhao, J. Shen, W. Yan, L. He, P.S. Thapa, S. Ren, B. Subramaniam, R.V. Chaudhari, Exceptional performance of bimetallic Pt1Cu3/TiO2 nanocatalysts for oxidation of gluconic acid and glucose with O2 to glucaric acid, Journal of Catalysis. 330 (2015) 323-329.
[57] O. Merino-Pérez, R. Martinez-Palou, J. Labidi, R. Luque, Microwave-Assisted Pretreatment of Lignocellulosic Biomass to Produce Biofuels and Value-Added Products, Biofuels and Biorefineries. 8 (2017) 30-33.
[58] S. Tabasso, G. Gravotto, Chapter 7Platform Chemicals from Biomass UsingMicrowave Irradiation, Biofuels and Biorefineries. 3 (2015).
[59] V.B. Kumar, I.N. Pulidindi, A. Gedanken, Synergistic catalytic effect of the ZnBr2–HCl system for levulinic acid production using microwave irradiation, RSC Advances. 5 (2015) 11043-11048.
[60] S. Maiti, G. Gallastegui, G. Suresh, V.L. Pachapur, S.K. Brar, Y. Le Bihan, P. Drogui, G. Buelna, M. Verma, R. Galvez-Cloutier, Microwave-assisted one-pot conversion of agro-industrial wastes into levulinic acid: An alternate approach, Bioresource Technology. 265 (2018) 471-479.
[61] S. Rautiainen, P. Lehtinen, M. Vehkamäki, K. Niemelä, M. Kemell, M. Heikkilä, T. Repo, Microwave-assisted base-free oxidation of glucose on gold nanoparticle catalysts, Catalysis Communications, 74 (2016) 115-118.
[62] L.-H. Gan, D. Deng, Y. Zhang, G. Li, X. Wang, L. Jiang, C.-R. Wang, Zn3V2O8 hexagon nanosheets: a high-performance anode material for lithium-ion batteries, Journal of Materials Chemistry A. 2 (2014) 2461-2466.
[63] J.L. Tingting Li, Zentaro Honda, Takeshi Fukuda, Norihiko Kamata, Sintering Condition and Optical Properties of Zn3V2O8Phosphor, Advances in Materials Physics and Chemistry. 2 (2012) 173-177
[64] L. Xiao, Y. Zhao, J. Yin, L. Zhang, Clewlike ZnV2O4 Hollow Spheres: Nonaqueous Sol–Gel Synthesis, Formation Mechanism, and Lithium Storage Properties, Chemistry – A European Journal. 15 (2009) 9442-9450.
[65]F. Mazloom, M. Masjedi-Arani, M. Ghiyasiyan-Arani, M. Salavati-Niasari, Novel sodium dodecyl sulfate-assisted synthesis of Zn3V2O8 nanostructures via a simple route, Journal of Molecular Liquids. 214 (2016) 46-53.
[66] F. Mazloom, M. Masjedi-Arani, M. Salavati-Niasari, Rapid and solvent-free solid-state synthesis and characterization of Zn3V2O8 nanostructures and their phenol red aqueous solution photodegradation, Solid State Sciences. 70 (2017) 101-109.
[67] C. Mondal, M. Ganguly, A.K. Sinha, J. Pal, R. Sahoo, T. Pal, Robust cubooctahedron Zn3V2O8 in gram quantity: a material for photocatalytic dye degradation in water, CrystEngComm. 15 (2013) 6745-6751.

[68] J. Bai, X. Li, G. Liu, Y. Qian, S. Xiong, Unusual Formation of ZnCo2O4 3D Hierarchical Twin Microspheres as a High-Rate and Ultralong-Life Lithium-Ion Battery Anode Material, Advanced Functional Materials. 24 (2014) 3012-3020.
[69] M. Shahid, J. Liu, Z. Ali, I. Shakir, M.F. Warsi, Structural and electrochemical properties of single crystalline MoV2O8 nanowires for energy storage devices, Journal of Power Sources. 230 (2013) 277-281.

[70] Y.T. Wang, A. Fang, X. X. Yang, Y. Yang, J. Luo, K. Xuo, G. Bao, One-step production of biodiesel from Jatropha oils with high acid value at low temperature by magnetic acid-base amphoteric nanoparticles, Chemical Engineering Journal. 348 (2018) 929-939.

[71] M.I. Alam, S. De, B. Singh, B. Saha, M.M. Abu-Omar, Titanium hydrogenphosphate: An efficient dual acidic catalyst for 5-hydroxymethylfurfural (HMF) production, Applied Catalysis A: General. 486 (2014) 42-48.

[72]H. Li, T. Yang, Z. Fang, Biomass-derived mesoporous Hf-containing hybrid for efficient Meerwein-Ponndorf-Verley reduction at low temperatures, Applied Catalysis B: Environmental. 227 (2018) 79-89.

[73] Y.T. Wang, Z. Fang, F. Zhang, Esterification of oleic acid to biodiesel catalyzed by a highly acidic carbonaceous catalyst, Catalysis Today. 319 (2019) 172-181.

[74] M. Mir, S.M. Ghoreishi, Response Surface Optimization of Biodiesel Production via Catalytic Transesterification of Fatty Acids, Chemical Engineering & Technology. 38 (2015) 835-834.
[75] H.-Y. Xu, S.-Y. Qi, Y. Li, Y. Zhao, J.-W. Li, Heterogeneous Fenton-like discoloration of Rhodamine B using natural schorl as catalyst: optimization by response surface methodology, Environmental Science and Pollution Research. 20 (2013) 5764-5772.
[764] L.C. Almeida, S. Garcia-Segura, N. Bocchi, E. Brillas, Solar photoelectro-Fenton degradation of paracetamol using a flow plant with a Pt/air-diffusion cell coupled with a compound parabolic collector: Process optimization by response surface methodology, Applied Catalysis B: Environmental. 103 (2011) 21-30.
[77] J. Herney-Ramirez, M. Lampinen, M.A. Vicente, C.A. Costa, L.M. Madeira, Experimental Design to Optimize the Oxidation of Orange II Dye Solution Using a Clay-based Fenton-like Catalyst, Industrial & Engineering Chemistry Research. 47 (2008) 284-294.
[78] A. Long, H. Zhang, Y. Lei, Surfactant flushing remediation of toluene contaminated soil: Optimization with response surface methodology and surfactant recovery by selective oxidation with sulfate radicals, Separation and Purification Technology. 118 (2013) 612-619.
[79] T. Xu, Y. Liu, F. Ge, L. Liu, Y. Ouyang, Application of response surface methodology for optimization of azocarmine B removal by heterogeneous photo-Fenton process using hydroxy-iron–aluminum pillared bentonite, Applied Surface Science. 280 (2013) 926-932.
[80] J. Wu, H. Zhang, N. Oturan, Y. Wang, L. Chen, M.A. Oturan, Application of response surface methodology to the removal of the antibiotic tetracycline by electrochemical process using carbon-felt cathode and DSA (Ti/RuO2–IrO2) anode, Chemosphere. 87 (2012) 614-620.
[81] Y. Hayashi, In Water or in the Presence of Water?, Angewandte Chemie International Edition. 45 (2006) 8103-8104.

[82] R. Wolfel, N. Taccardi, A. Bosmann, P. Wasserscheid, Selective catalytic conversionof biobased carbohydrates to formic acid using molecular oxygen, Green chem. 13 (2011) 2759–2763

[83] M.Imbierowicz, M.Troszkiewicz, K.Piotrowska, Heat effects of wet oxidation of glucose: A biomass model compound, Chemical engineering journal. 260 (2015) 864-874

[84] I. V.Delidovich,B. L.Moroz, O. P.Taran, ,N. V.Gromov, P. A.Pyrjaev, I. P.Prosvirin, V. I.Bukhtiyarov, V. N.Parmon, Aerobic selective oxidation of glucose to gluconate catalyzed by Au/Al2O3and Au/C: Impact of the mass-transfer processes on the overall kinetics, Chemical engineering journal. 223 (2013) 921-931.

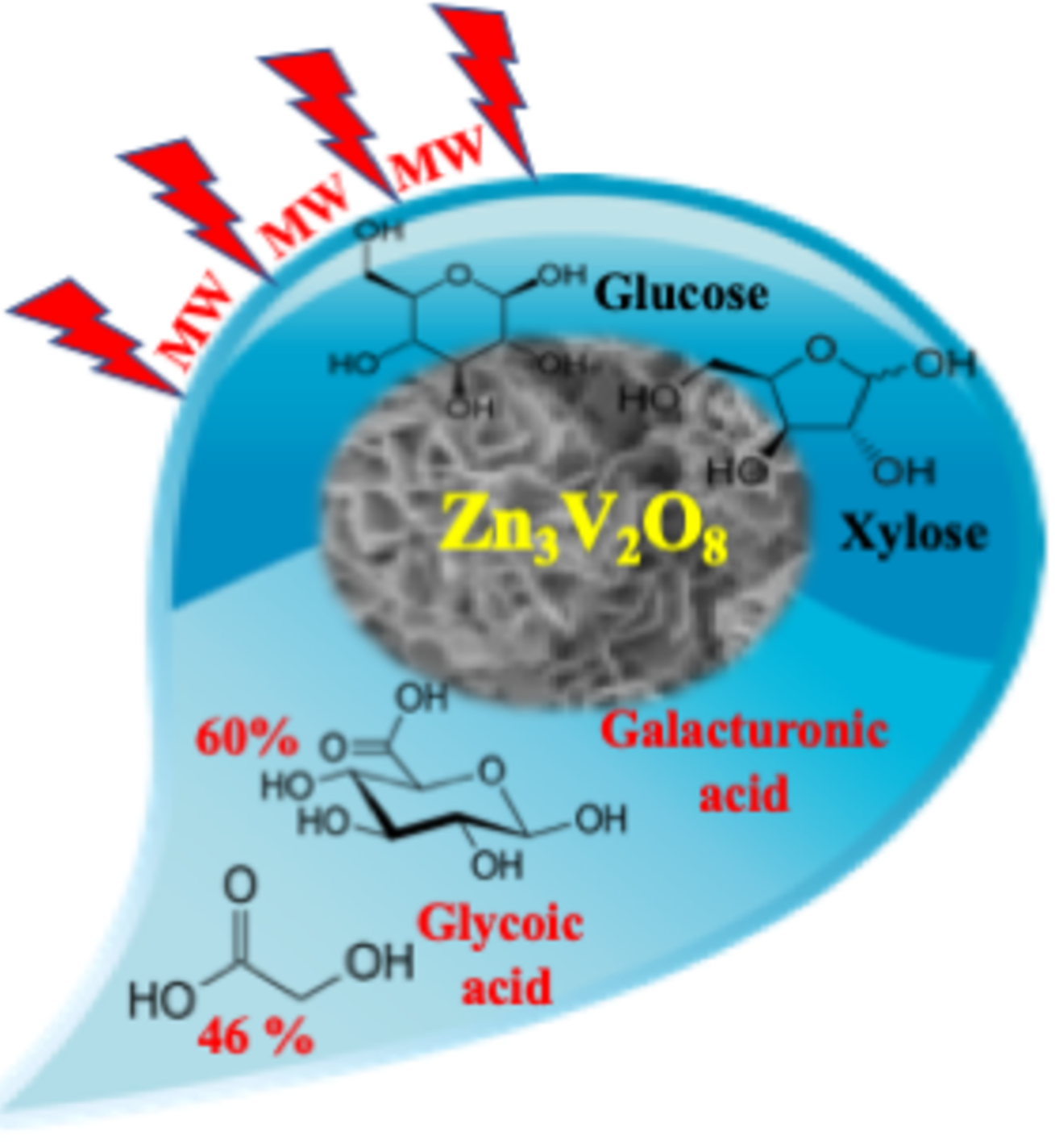
MW
MW
MW
Glucose
Xylose
$Zn_3V_2O_8$
60%
Galacturonic acid
Glycoic acid
46 %